ACS APPLIED BIO MATERIALS
Cite This: ACS Appl. Bio Mater. 2020, 3, 1158−1164
Article
www.acsabm.org

Electrochemiluminescence Biosensor for Hyaluronidase Based on the $Ru(bpy)_3^{2+}$ Doped SiO_2 Nanoparticles Embedded in the Hydrogel Fabricated by Hyaluronic Acid and Polyethylenimine

Zhixin Li,[†] Jinwei Zhang,[†] Huixing Chen,[‡] Xiaocui Huang,[†] Da Huang,[§] Fang Luo,[§] Jian Wang,*[,†] Longhua Guo,[†] Bin Qiu,[†] and Zhenyu Lin*[,†]

[†]Ministry of Education Key Laboratory for Analytical Science of Food Safety and Biology, Fujian Provincial Key Laboratory of Analysis and Detection for Food Safety, College of Chemistry, and [§]College of Biological Science and Engineering, Fuzhou University, Fuzhou, Fujian 350116, China

[‡]Department of Hepatobiliary Surgery, Fujian Medical University Union Hospital, Fuzhou, Fujian 350000, China

ABSTRACT: Hyaluronidase (HAase), a specific enzyme of hyaluronic acid (HA), has been reported as a potential tumor biomarker in recent years. Hence, developing some simple, rapid, and sensitive methods for HAase assay is necessary. In this work, a simple and sensitive biosensor constructed by a reliable controlled release system and a mature electrochemiluminescence (ECL) analytical technique has been devised for the quantification of HAase with high efficiency and selectivity. Tris (2,2′-bipyridyl) ruthenium(II) chloride hexahydrate doped SiO_2 nanoparticles ($Ru@SiO_2$ NPs), as ECL signal probes, were trapped in the hydrogel fabricated by HA and polyethylenimine evenly and steadily. When HAase existed, the hydrogel was decomposed by HAase, and the $Ru@SiO_2$ NPs escaped from the hydrogel into the supernate. The ECL signal produced from the supernate can be detected and used to characterize HAase concentration. The result showed a good linear relationship between ECL intensity, and HAase concentration ranged from 2 to 60 U/mL and the limit of detection was 2 U/mL. The developed controlled release ECL biosensor has been used for HAase quantification in urine samples with satisfactory results.

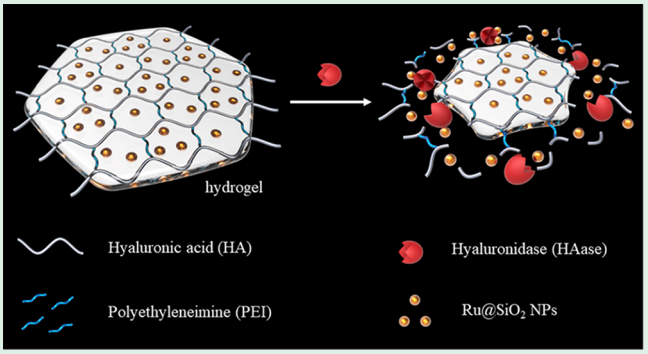

KEYWORDS: *controlled release, electrochemiluminescence, hyaluronidase, hyaluronic acid, polyethylenimine, hydrogel*

INTRODUCTION

Controlled released systems can change their physicochemical properties in response to specific stimuli, such as pH,[1] temperature,[2] acoustics,[3] voltage,[4] light,[5,6] molecules,[7] and so on. Plentiful controlled release systems based on hydrogel,[1,8−10] mesoporous silica nanoparticle,[11,12] metal−organic framework,[13−15] liposomes,[3,16] nanomaterials,[17] and so on have been designed and widely used in intelligent drug delivery and targeted cancer therapy because of their outstanding loading capacity and stimuli-responsive capability. Recently, controlled release systems had been coupled with diverse detection techniques to develop biosensors for different targets.[11,18−21] Electrochemiluminescence (ECL), a kind of electrogenerated chemiluminescence phenomenon, has the advantages of low background signal, high sensitivity, and inexpensive measuring equipment because it does not require external light sources.[22,23] To the best of our knowledge, little attention has been paid to developing a biosensor that combined the superiorities of a controlled release system and ECL detection, although these sensors may have the advantages of simple construction and outstanding signal probe loading capacity, sensitivity, and selectivity.

Hyaluronidase (HAase), an enzyme that can hydrolyze hyaluronic acid (HA) with high efficiency, has been reported as a tumor biomarker in recent years. Excessive HAase has been reported as relevant to some malignancies at the early stages.[24−26] In addition, HAase has also been widely applied to reduce the increased intraocular pressure caused by HA in cosmetic surgery and eye surgery.[27] The right amount of HAase can accelerate the spread of anesthetics in tissues through decomposing HA, but sometimes excess HAase may cause allergies.[28−30] Therefore, measuring HAase with high accuracy is of great importance. Many methods, including fluorescent methods,[31−39] colorimetric methods,[40,41] and weighting methods,[42] have been developed for the determination of HAase so far. Our group has reported an ECL method for HAase detection,[43] HA-tris (2,2′-bipyridyl) ruthenium(II) chloride hexahydrate ($Ru(bpy)_3^{2+}$) complex was fabricated by $Ru(bpy)_3^{2+}$ and macromolecular HA through electrostatic interaction, which can be cleaved by HAase into

Received: November 24, 2019
Accepted: December 24, 2019
Published: December 24, 2019

DOI: 10.1021/acsabm.9b01082
ACS Appl. Bio Mater. 2020, 3, 1158−1164

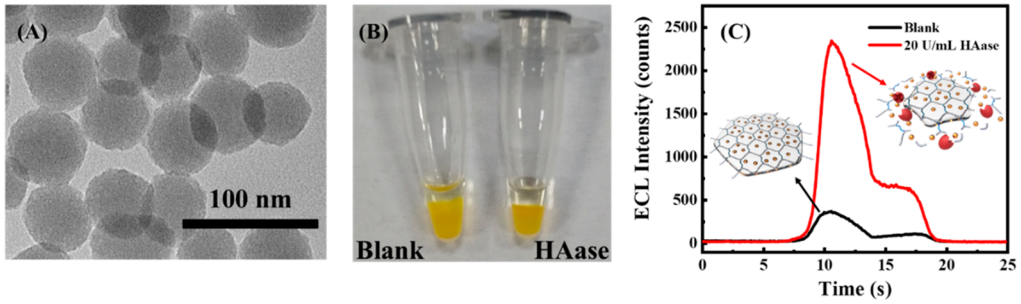

Figure 1. (A) TEM image of $Ru@SiO_2$ NPs. (B) Hydrogel and residual supernate of control group and experimental group after the enzymatic hydrolysis reaction and (C) The ECL signal of control group and experimental group (20 U/mL HAase) detected by the proposed ECL hydrogel biosensor.

Scheme 1. Principle of the Controlled Release ECL Biosensor for HAase Detection

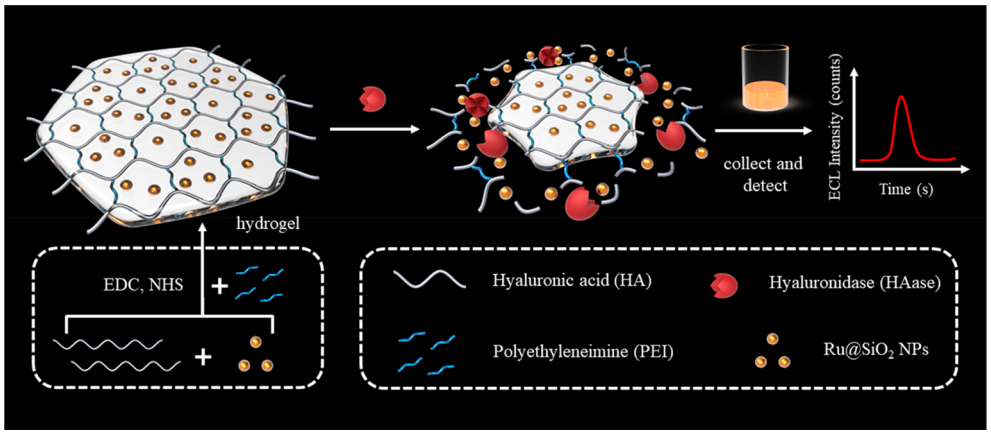

small pieces and collected for HAase quantification. However, some free $Ru(bpy)_3^{2+}$ existed in solution that kept balance with the $Ru(bpy)_3^{2+}$ on an HA-$Ru(bpy)_3^{2+}$ complex, which caused a strong background signal; therefore, a cumbersome centrifugal process is needed for reducing the background signal. Efforts need to be made to address these problems.

In this work, a novel controlled release ECL biosensor has been devised to quantify HAase concentration. The controlled release system is designed on the basis of the hydrogel constructed by HA and polyethylenimine (PEI), and a large number of $Ru(bpy)_3^{2+}$-doped SiO_2 nanoparticles ($Ru@SiO_2$ NPs) were trapped in the hydrogel steadily as ECL signal probes. When HAase existed, the hydrogel was decomposed by HAase, and $Ru@SiO_2$ NPs escaped from the hydrogel to supernate. The ECL signal produced from the supernate can be detected and used to characterize HAase concentration. Compared with the previous work, the proposed system does not require abundant HA for signal probe immobilizing, and a cumbersome centrifugal process for background interference reduction is not required. The developed method has been applied in quantitative analysis of HAase concentration quantification in urine samples with high sensitivity and selectivity.

EXPERIMENTAL SECTION

Materials. $Ru(bpy)_3^{2+}$, HAase, HA, tripropylamine (TPA), and alkaline phosphatase (ALP) were acquired from Sigma-Aldrich (Shanghai, China). *N*-hydroxy succinimide (NHS), uric acid (UA), bovine serum albumin (BSA), 1-(3-(dimethylamino)propyl)-3-ethyl-carbodiimide (EDC), PEI, and glutathione (GSH) were acquired from Aladdin Bio-Chem Technology Co., Ltd. (Shanghai, China). Ethanol, tetraethyl orthosilicate (TEOS), $CaCl_2$ and $MgCl_2$ were purchased from Sinopharm Chemical Reagent Co., Ltd. 20× phosphate buffered saline (0.2 M) was acquired from Sangon Biotechnology Co., Ltd. (Shanghai, China). NaCl, KCl, urea, and glucose (Glu) were acquired from Xilong Scientific Co., Ltd. (Guangdong, China). Deionized water (Milli-Q, Millipore, 18.2 MΩ·cm) was used for solution preparation throughout the experiment.

Apparatus. ECL intensity was measured by a laboratory made system composed of a BPCL ultraweak luminescence analyzer (Institute of Biophysics, Chinese Academy of Science, Beijing, China) for ECL detection and a CHI660D electrochemical workstation (Chenhua Instruments, Shanghai, China) for electrochemical measurements. A three-electrode system including glassy carbon electrode (working electrode), platinum wire electrode (counter electrode), and an Ag/AgCl (reference electrode, saturated with KCl) electrode was purchased from Gaoss Union Technology Ltd. (Wuhan, China).

Synthesis of $Ru@SiO_2$ NPs. The $Ru@SiO_2$ NPs were prepared referring to our early reported procedures.[44] Two milliliters of H_2O, 5 μL of 10.0 mM $Ru(bpy)_3^{2+}$, and a solution of a 50 mL portion of ethanol were mixed evenly in a 100 mL beaker. Then 1.6 mL of $NH_3 \cdot H_2O$ was added in the beaker. After that, 1.5 mL of TEOS was injected slowly into the mixture solution, and plastic film was used to seal the mouth of the beaker. The whole reaction process was performed at room temperature with magnetic stirring for 24 h. The $Ru@SiO_2$ NPs were centrifuged at 8000 rpm, washed with ethanol, and rinsed with deionized water three times, respectively. Finally, the $Ru@SiO_2$ NPs were dissolved in deionized water for later use. A TEM image of $Ru@SiO_2$ NPs is shown in Figure 1A. The size of the $Ru@SiO_2$ NPs was about 50 nm, indicating that $Ru@SiO_2$ NPs with even size have been synthesized in this work.

Assembly of ECL Hydrogel Containing $Ru@SiO_2$ NPs. $Ru@SiO_2$ NP solution (4 μL, 10 mg/mL) was mixed with H_2O (2 μL) and

DOI: 10.1021/acsabm.9b01082
ACS Appl. Bio Mater. 2020, 3, 1158−1164

HA sodium salt solution (4 μL, 10 mg/mL) in centrifuge tube (200 μL) first. Next, EDC solution (48.8 mg/mL, 2 μL) and NHS solution (11.5 mg/mL, 2 μL) were dropped to the mixed solution to activate the carboxyl groups of HA for 15 min. Then PEI solution (2 μL, 4 mg/mL) was injected into the mixture solution with rapid oscillation for 2 h (350 rpm). After that, deionized H_2O (0.1 mL) was dropped on the hydrogel and allowed to stand for 10 min to clean the surface of the hydrogel and the wall of centrifuge tube. Finally, the H_2O was cleaned up by filter paper, and the clean hydrogel was obtained in a centrifugal tube (kept in a dark place) for later use.

Procedures for HAase Quantification. HAase solutions (60 μL) with different concentration were dropped on the top of the aforesaid hydrogel in centrifugal tubes, respectively. Centrifugal tubes were then kept in a dark place and shaken at 37 °C for 2 h (350 rpm) to make HAase decompose into the hydrogel. Afterward, 50 μL of supernate was gathered and dissolved in phosphate buffered saline (0.01 M, 2 mL) containing 8 μL of TPA for ECL detection. The ECL signal was recorded with the scanning potential range from 0.4 to 1.6 V, the scan rate was set at 100 mV/s, and photomultiplier tube voltage was set at −800 V.

RESULTS AND DISCUSSION

Principle of Controlled Release ECL Biosensor for HAase Quantification. The principle of controlled release ECL biosensor is depicted in Scheme 1. The signal molecule $Ru@SiO_2$ NPs was preliminarily incorporated into the HA solution before the synthesis of the hydrogel, followed by the addition of EDC and NHS to activate the carboxyl groups of HA. Finally, amino PEI was added to form a hydrogel by forming plenty of amide bond with HA. When there was no HAase, the hydrogel remained stable, and the $Ru@SiO_2$ NPs trapped in the hydrogel can hardly escape from the hydrogel, and therefore, only a weak ECL signal was recorded from the supernatant. When HAase was present, HAase can decompose the hydrogel by enzymatic hydrolysis of HA in the hydrogel. $Ru@SiO_2$ NPs escaped from the ruptured hydrogel to the supernatant. The supernatant was collected and used for ECL detection. The ECL intensity from the supernatant is relevant to HAase activity, by this means, a simple but sensitive method for HAase which combined the merits of controlled release system and ECL detection technique can be developed.

A simple controlled trial was performed to confirm the feasibility of the above-mentioned speculation. The result was depicted in Figure 1B, C, in experimental group (20 U/mL HAase), the volume of hydrogel decreased and volume of supernatant increased, and the supernatant turned yellow because of the escaping of $Ru@SiO_2$ NPs from hydrogel. Moreover, a strong ECL signal produced from the supernatant was recorded (curve a), further indicating plenty of $Ru@SiO_2$ NPs escaped from ruptured hydrogel caused by HAase. However, in control group, the volume of hydrogel and colorless supernatant was nearly no change, and only a weak ECL signal was recorded (curve b), which might be caused by trace number of $Ru@SiO_2$ NPs escaped from the hydrogel surface. All these phenomena demonstrated the principle of the proposed assay is feasible.

Optimization of the Conditions. The network structure density of hydrogel has great effects on the performance of the proposed biosensor. Low density of network structure can make the hydrogel break down through enzymolysis easily, but $Ru@SiO_2$ NPs can escape from the hydrogel to the supernatant, which may cause a large background signal. The high density of the network structure can make $Ru@SiO_2$ NPs steadily embed in the hydrogel, resulting in a high signal-to-noise ratio. However, it can also make the hydrogel too stable to be decomposed by HAase, leading to a low sensitivity. Therefore, two vital experimental conditions (quantity of PEI in hydrogel and water content of hydrogel) which can affect the network structure density of hydrogel were investigated to obtain the optimal experimental conditions.

The quantity of PEI was first optimized. Large quantity of PEI added to synthesis hydrogel means that plenty of amide bonds will be formed in the hydrogel, which can cause a hydrogel with high density of network structure. As shown in Figure 2A, the ECL intensity of experimental group and

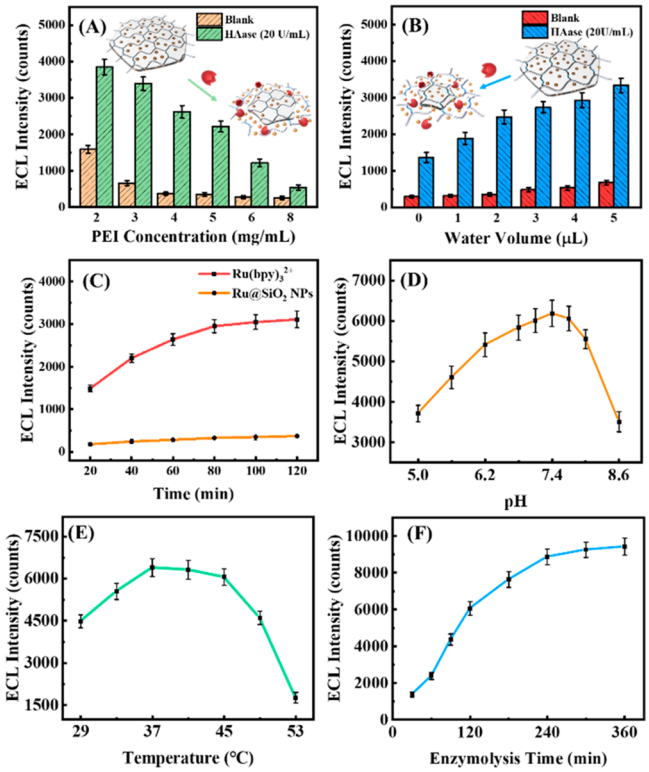

Figure 2. (A) Effect of the hydrogel biosensor synthesized by different concentration of PEI (2−8 mg/mL) on the ECL intensity at HAase (20 U/mL) detection process. (B) Effect of the hydrogel biosensor with different water contents on the ECL intensity at HAase (20 U/mL) detection process. Different volumes of water (1−7 μL) were added to optimize the water content of the hydrogel. (C) The leakage of $Ru(bpy)_3^{2+}$ and $Ru@SiO_2$ NPs embedded in the hydrogel during 2 h. (D) Effect of pH (5.0−8.6) on ECL intensity at HAase (40 U/mL) detection process. (E) Effect of temperature (29−53 °C) on ECL intensity at HAase (40 U/mL) detection process. (F) Effect of enzymolysis time (0.5−6 h) on ECL intensity at HAase (40 U/mL) detection process. Error bars represent the standard deviations for three replicates, the same below.

control group increased with the decrease of PEI quantity. It indicated that the hydrogel with low density of network structure can make $Ru@SiO_2$ NPs escaped from the hydrogel easily through HAase enzymolysis, and meanwhile, low density of network structure can also make more $Ru@SiO_2$ NPs leak out of the hydrogel without HAase, and cause a high background signal. To obtain high signal-to-noise ratio hydrogel biosensor, we chose 4 mg/mL PEI (2 μL) involved in the synthesis of hydrogel as the optimal experimental condition.

The water content of the hydrogel can also influence the density of the hydrogel network structure. High water content

DOI: 10.1021/acsabm.9b01082
ACS Appl. Bio Mater. 2020, 3, 1158−1164

of the hydrogel results in the low density of network structure in hydrogel because of a low concentration of HA and PEI in hydrogel. To optimize the water content of the hydrogel, we added different volumes of water to participate in the synthesis of hydrogels. As depicted in Figure 2B, the ECL signal of experimental group and control group increased gradually as the water content of the hydrogel increased, indicating that high water content of hydrogel can improve the enzymolysis efficiency, and at the same time, more Ru@SiO_2 NPs can escape from the hydrogel without HAase and cause a high background signal. Therefore, to obtain a high signal-to-noise ratio hydrogel biosensor, we added 2 μL of H_2O to take part in the fabrication of hydrogels.

In addition, ECL signal probes with different sizes have great influence in the leakage of the hydrogel. High leakage can cause a high background signal and low sensitivity. Therefore, Ru@SiO_2 NPs and $Ru(bpy)_3^{2+}$ have been embedded in the hydrogel to evaluate the leakage of the proposed controlled released system. As shown in Figure 2C, the ECL signal of the supernate from the hydrogel containing $Ru(bpy)_3^{2+}$ (small molecule) was higher than that from the hydrogel containing Ru@SiO_2 NPs (about 50 nm), and the change in the ECL signal over 2 h from the hydrogel containing $Ru(bpy)_3^{2+}$ is also bigger, indicating that the network structure of the hydrogel cannot prevent $Ru(bpy)_3^{2+}$ from escaping because of the small size of the $Ru(bpy)_3^{2+}$. Therefore, Ru@SiO_2 NPs was chosen as the optimized ECL signal probe for the controlled-release ECL biosensor fabrication.

The temperature and pH during the enzymolysis reaction, which have great influence on the property of the controlled release ECL biosensor, have been optimized. Figure 2D shows that the ECL intensity increased first when the temperature increased from 29 to 37 °C and peaked at 37 °C, then decreased with a temperature over 37 °C, indicating that 37 °C was the optimized temperature for hydrogel breaking down. Similarly, as depicted in Figure 2E, the ECL intensity increased when the pH value increased from 5.0 to 7.4 and peaked at 7.4, and finally decreased when the pH value was greater than 7.4, indicating that pH 7.4 was the optimal condition for hydrogel breaking down.

An appropriate enzymolysis time is also a key factor of the property of the proposed biosensor. Short enzymolysis time can enhance the detection efficiency of the biosensor on the one hand while reducing its sensitivity on the other. As depicted in Figure 2F, the ECL intensity increased rapidly with the enzymolysis time increased from 0.5 to 2 h, then increased slowly with the enzymolysis time increased from 2 to 4 h, and finally tended to be stable after 4 h. Therefore, 2 h was selected as the most suitable enzymolysis time that can detect HAase concentration sensitively and efficiently.

Performance of the Controlled Release ECL Biosensor. The quantitative experiment of the controlled release ECL biosensor was carried out by the addition of different concentration of HAase into the system. As shown in Figure 3A, the ECL intensity increased with increasing HAase concentration. There is a linear relationship between ECL intensity and the concentration of HAase ranged from 2 to 60 U/mL (Figure 3 B). The linear equation is

$$I_{ECL}/(\text{counts}) = 143.34C_{HAase}/(\text{U/mL}) + 208.88R = 0.9958$$

where I_{ECL} is the ECL intensity detected by the biosensor in different HAase concentrations, C_{HAase} is the HAase concentration, and R is the correlation coefficient. The limit of detection (LOD) was 2 U/mL, which can meet practical detection requirements. If a lower concentration of HAase needsto be detected, enzymolysis time can be extended to obtain a lower LOD, similar to our previous work.[42]

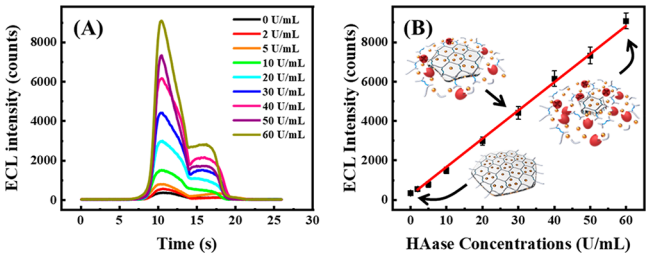

Figure 3. (A) ECL response at different HAase concentrations (2−60 U/mL). (B) The linear relationship between ECL intensity and the HAase concentrations.

Compared to most of the other methods (Table 1), the proposed method has high sensitivity and wide liner range, and the novel biosensor can be fabricated easily and used for HAase detection with high efficiency. Especially when compared with our early reported ECL methods,[43] the proposed method has lower background signal, higher signal-to-noise ratio, wider linear range, shorter detection time, anda brief preparation process without cumbersome centrifugal.

Table 1. Comparison of Different Methods for HAase Detection

method	linear range (U/mL)	LOD (U/mL)	detection time (min)	ref
colorimetric		2.4	65	32
fluorescence	1.25−50	0.625	180	31
fluorescence & colorimetric	0.1−80	0.06	120	33
fluorescence	1−50	0.7	45	36
fluorescence	0.025−0.2	0.007	90	Biosensors and Bioelectronics 79 (2016) 776−783
fluorescence	0.1−8	0.05	96	37
ECL	2.0−40	0.33	150	43
fluorescence	two sections, 0.05−2 and 2.75−5	0.02	100	38
fluorescence	0.5−37.5	0.30	65	39
weighting	1.0−60	1.0	210	42
	0.2−10	0.20	330	
ECL with controlled release system	2.0−60	2.0	120	this work

The selectivity of the above-mentioned biosensor was tested by detecting various potential interfering substances at the optimized conditions and depicted in Figure 4. Compared with HAase, all these interfering substances revealed little effect on ECL response, indicating that the proposed biosensor has high selectivity.

Hydrogel containing Ru@SiO_2 NPs had been prepared and kept in dark place at 4 °C for later use, and had been used to detect 40 U/mL of HAase every week. The results showed that after 4 weeks' storage, nearly no change was observed as compared with the freshly prepared one, indicating that the prepared hydrogel containing Ru@SiO_2 NPs has good stability.

DOI: 10.1021/acsabm.9b01082
ACS Appl. Bio Mater. 2020, 3, 1158−1164

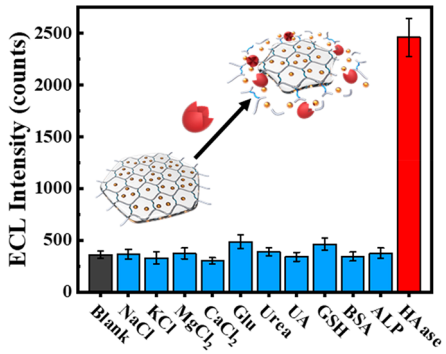

Figure 4. Controlled release ECL biosensor responded to HAase and different interferences, including NaCl (10 mM), KCl (10 mM), $MgCl_2$ (10 mM), $CaCl_2$ (10 mM), Glu (10 mM), urea (10 mM), UA (10 mM), GSH (10 mM), BSA (1 mM), ALP (10 mM), and HAase (20 U/mL).

Application of the Controlled Release ECL Biosensor. HAase in urine samples were measured by controlled release ECL biosensor and commercial enzyme linked immunosorbent assay (ELISA) kit (for a comparison) to tested the property of the proposed biosensor (donated from volunteers, including cancer patients and healthy individuals). The results (Table 2)

Table 2. Quantification of HAase Activity in Urine Samples with Controlled Release ECL Biosensor (n = 3)

urine samples		spiked (U/mL)	detected HAase by current method (U/mL)	detected HAase by ELISA method (U/mL)	recovery rate (%)	RSD (%)
healthy individuals	1	0	2.87	3.05		5.61
		10.0	12.28	13.03	94.11	8.78
		20.0	23.77	22.89	104.53	6.44
		30.0	33.69	33.17	102.72	4.80
	2	0	3.04	3.01		6.48
		10.0	13.54	13.03	104.95	4.02
		20.0	23.50	22.95	102.30	6.69
		30.0	34.48	33.26	104.80	5.73
	3	0	3.45	3.49		5.77
		10.0	14.13	13.44	106.81	6.07
		20.0	23.57	23.49	100.61	5.34
		30.0	34.33	33.62	102.95	2.59
cancer patients	1	0	25.73	26.47		5.02
		10.0	35.60	36.58	98.69	4.74
		20.0	47.07	46.42	106.67	3.61
		30.0	57.67	56.75	106.44	4.25
	2	0	36.44	36.16		5.41
		10.0	46.55	46.03	101.08	2.99
		20.0	57.21	56.58	103.84	4.78
		30.0	66.16	66.49	99.06	3.02
	3	0	43.68	42.94		6.54
		10.0	53.66	52.75	99.82	4.49
		20.0	64.61	63.23	104.66	1.40
		30.0	74.22	72.86	101.80	4.88

showed that the HAase concentration of urine samples from healthy individuals (2.87, 3.04, and 3.45 U/mL) was much less than that from cancer patients (25.73, 36.44, and 43.68 U/mL), and the proposed method has no significant difference with the ELISA method. In addition, the standard addition recovery was tested to evaluated the proposed biosensor accuracy. The result shows that the recovery rates ranged from 94.11 to 106.81%, and the relative standard deviation (RSD, n = 3) is less than 8.78%, indicating that the proposed biosensor can quantify HAase in complex biological samples effectively and reliably.

CONCLUSION

In summary, an enzyme-responding, controlled-release ECL hydrogel biosensor has been devised for HAase quantification. The developed biosensor combined the advantages of excellent sensitivity of ECL detection and outstanding loading capacity of stimuli-responsive controlled release system and has been used for HAase activity assay in urine samples. To the best of our knowledge, it is the first report that a biosensor can be constructed by the ECL analytical technique and the reliable controlled release system for HAase detection with satisfactory results, demonstrating that the developed strategy puts forward a new path for designing high-efficiency ECL biosensors and has a great potential in bioanalysis. In addition, because PEI can be replaced with target-responsive amino probes (such as double strand amino-modified DNA) for hydrogel fabrication, the hydrogel shows outstanding universality and extendibility that can be widely used to design controlled release ECL biosensors for various biomarkers' detection.

AUTHOR INFORMATION

Corresponding Authors

*Email: jwang@fzu.edu.cn.Phone/fax: 86-591-22866135 (J.W.).
*Email: zylin@fzu.edu.cn (Z.L.) .

ORCID

Fang Luo: 0000-0003-1480-0677
Longhua Guo: 0000-0003-0706-0973
Zhenyu Lin: 0000-0001-7890-6812

Notes

The authors declare no competing financial interest.

ACKNOWLEDGMENTS

This project was financially supported by National Sciences Foundation of China (21775026, 21575025, 21575027), the Program for Changjiang Scholars and Innovative Research Team in University (IRT15R11) and the cooperative project of production and study in University of Fujian Province (2018Y4007), the Sciences Foundation of Fujian Province (2018J01685, 2018J01682), STS Key Project of Fujian Province (2017T3007).

REFERENCES

(1) Liang, Y. P.; Zhao, X.; Ma, P. X.; Guo, B. L.; Du, Y. P.; Han, X. Z. pH-responsive injectable hydrogels with mucosal adhesiveness based on chitosan-grafted-dihydrocaffeic acid and oxidized pullulan for localized drug delivery. *J. Colloid Interface Sci.* **2019**, *536*, 224–234.

(2) Li, W.; Huang, L.; Ying, X.; Jian, Y.; Hong, Y.; Hu, F.; Du, Y. Antitumor Drug Delivery Modulated by A Polymeric Micelle with an Upper Critical Solution Temperature. *Angew. Chem., Int. Ed.* **2015**, *54* (10), 3126–3131.

(3) Lu, Y.; de Vries, W. C.; Overeem, N. J.; Duan, X.; Zhang, H.; Zhang, H.; Pang, W.; Ravoo, B. J.; Huskens, J. Controlled and Tunable Loading and Release of Vesicles by Using Gigahertz Acoustics. *Angew. Chem., Int. Ed.* **2019**, *58* (1), 159–163.

DOI: 10.1021/acsabm.9b01082
ACS Appl. Bio Mater. 2020, 3, 1158–1164

(4) Liu, S.; Fu, Y.; Li, G.; Li, L.; Law, H. K.-w.; Chen, X.; Yan, F. Conjugated Polymer for Voltage-Controlled Release of Molecules. *Adv. Mater.* **2017**, *29* (35), 1701733.
(5) Paret, N.; Trachsel, A.; Berthier, D. L.; Herrmann, A. Controlled Release of Encapsulated Bioactive Volatiles by Rupture of the Capsule Wall through the Light-Induced Generation of a Gas. *Angew. Chem., Int. Ed.* **2015**, *54* (7), 2275−2279.
(6) Deng, H.; Lin, L.; Wang, S.; Yu, G.; Zhou, Z.; Liu, Y.; Niu, G.; Song, J.; Chen, X. X-ray-Controlled Bilayer Permeability of Bionic Nanocapsules Stabilized by Nucleobase Pairing Interactions for Pulsatile Drug Delivery. *Adv. Mater.* **2019**, *31* (37), 1903443.
(7) Ma, Y.; Wang, Z.; Ma, Y.; Han, Z.; Zhang, M.; Chen, H.; Gu, Y. A Telomerase-Responsive DNA Icosahedron for Precise Delivery of Platinum Nanodrugs to Cisplatin-Resistant Cancer. *Angew. Chem., Int. Ed.* **2018**, *57* (19), 5389−5393.
(8) Gao, S.; Tang, G.; Hua, D.; Xiong, R.; Han, J.; Jiang, S.; Zhang, Q.; Huang, C. Stimuli-responsive bio-based polymeric systems and their applications. *J. Mater. Chem. B* **2019**, *7* (5), 709−729.
(9) Dimatteo, R.; Darling, N. J.; Segura, T. In situ forming injectable hydrogels for drug delivery and wound repair. *Adv. Drug Delivery Rev.* **2018**, *127*, 167−184.
(10) Li, J.; Mo, L.; Lu, C.-H.; Fu, T.; Yang, H.-H.; Tan, W. Functional nucleic acid-based hydrogels for bioanalytical and biomedical applications. *Chem. Soc. Rev.* **2016**, *45* (5), 1410−1431.
(11) Fan, D.; Li, N.; Ma, H.; Li, Y.; Hu, L.; Du, B.; Wei, Q. Electrochemical immunosensor for detection of prostate specific antigen based on an acid cleavable linker into MSN-based controlled release system. *Biosens. Bioelectron.* **2016**, *85*, 580−586.
(12) Yang, P.; Gai, S.; Lin, J. Functionalized mesoporous silica materials for controlled drug delivery. *Chem. Soc. Rev.* **2012**, *41* (9), 3679−3698.
(13) Abánades Lázaro, I.; Forgan, R. S. Application of zirconium MOFs in drug delivery and biomedicine. *Coord. Chem. Rev.* **2019**, *380*, 230−259.
(14) Wu, M. X.; Yang, Y. W. Metal-Organic Framework (MOF)-Based Drug/Cargo Delivery and Cancer Therapy. *Adv. Mater.* **2017**, *29* (23), 20.
(15) Chen, X. R.; Tong, R. L.; Shi, Z. Q.; Yang, B.; Liu, H.; Ding, S. P.; Wang, X.; Lei, Q. F.; Wu, J.; Fang, W. J. MOF Nanoparticles with Encapsulated Autophagy Inhibitor in Controlled Drug Delivery System for Antitumor. *ACS Appl. Mater. Interfaces* **2018**, *10* (3), 2328−2337.
(16) He, H.; Lu, Y.; Qi, J.; Zhu, Q.; Chen, Z.; Wu, W. Adapting liposomes for oral drug delivery. *Acta Pharm. Sin. B* **2019**, *9* (1), 36−48.
(17) Qiu, J.; Huo, D.; Xue, J.; Zhu, G.; Liu, H.; Xia, Y. Encapsulation of a Phase-Change Material in Nanocapsules with a Well-Defined Hole in the Wall for the Controlled Release of Drugs. *Angew. Chem., Int. Ed.* **2019**, *58* (31), 10606−10611.
(18) Lin, B.; Liu, D.; Yan, J.; Qiao, Z.; Zhong, Y.; Yan, J.; Zhu, Z.; Ji, T.; Yang, C. J. Enzyme-Encapsulated Liposome-Linked Immunosorbent Assay Enabling Sensitive Personal Glucose Meter Readout for Portable Detection of Disease Biomarkers. *ACS Appl. Mater. Interfaces* **2016**, *8* (11), 6890−6897.
(19) Wei, X.; Tian, T.; Jia, S.; Zhu, Z.; Ma, Y.; Sun, J.; Lin, Z.; Yang, C. J. Microfluidic Distance Readout Sweet Hydrogel Integrated Paper-Based Analytical Device (μDiSH-PAD) for Visual Quantitative Point-of-Care Testing. *Anal. Chem.* **2016**, *88* (4), 2345−2352.
(20) Zhu, Z.; Guan, Z.; Jia, S.; Lei, Z.; Lin, S.; Zhang, H.; Ma, Y.; Tian, Z.-Q.; Yang, C. J. Au@Pt Nanoparticle Encapsulated Target-Responsive Hydrogel with Volumetric Bar-Chart Chip Readout for Quantitative Point-of-Care Testing. *Angew. Chem., Int. Ed.* **2014**, *53* (46), 12503−12507.
(21) Qiu, Z. L.; Shu, J.; Tang, D. P. Bioresponsive Release System for Visual Fluorescence Detection of Carcinoembryonic Antigen from Mesoporous Silica Nanocontainers Mediated Optical Color on Quantum Dot-Enzyme-Impregnated Paper. *Anal. Chem.* **2017**, *89* (9), 5152−5160.
(22) Hu, L.; Xu, G. Applications and trends in electrochemiluminescence. *Chem. Soc. Rev.* **2010**, *39* (8), 3275−3304.
(23) Li, L.; Chen, Y.; Zhu, J.-J. Recent Advances in Electrochemiluminescence Analysis. *Anal. Chem.* **2017**, *89* (1), 358−371.
(24) Martinez-Quintanilla, J.; He, D.; Wakimoto, H.; Alemany, R.; Shah, K. Encapsulated Stem Cells Loaded With Hyaluronidase-expressing Oncolytic Virus for Brain Tumor Therapy. *Mol. Ther.* **2015**, *23* (1), 108−118.
(25) Mladkova, J.; Sanda, M.; Matouskova, E.; Selicharova, I., Phenotyping breast cancer cell lines EM-G3, HCC1937, MCF7 and MDA-MB-231 using 2-D electrophoresis and affinity chromatography for glutathione-binding proteins. *BMC Cancer* **2010**, *10*. DOI: 10.1186/1471-2407-10-449
(26) Benitez, A.; Yates, T. J.; Lopez, L. E.; Cerwinka, W. H.; Bakkar, A.; Lokeshwar, V. B. Targeting Hyaluronidase for Cancer Therapy: Antitumor Activity of Sulfated Hyaluronic Acid in Prostate Cancer Cells. *Cancer Res.* **2011**, *71* (12), 4085−4095.
(27) Xu, Q.; Zhou, H.; Luo, M.; Fan, X. The effect of hyaluronidase on intraocular pressure and indirect orbital tension following retrobulbar anesthesia. *Chin. J. Pract. Ophthalmol.* **2004**, *22* (4), 263−265.
(28) Rajalakshmi, A. R.; Kumar, M. A. Hyaluronidase hypersensitivity: A rare complication of peribulbar block. *Indian J. Ophthalmol.* **2016**, *64* (2), 160.
(29) Raichura, N. D.; Alam, M. S.; Jaichandran, V. V.; Mistry, S.; Mukherjee, B. Hyaluronidase allergy mimicking orbital cellulitis. *Orbit* **2018**, *37* (2), 149−153.
(30) Alcubierre, R.; Sanchez-Dalmau, B. F.; Mousavi, K. Compressive optic neuropathy secondary to an allergic reaction to hyaluronidase. *Archivos de la Sociedad Española de Oftalmología (English Edition)* **2019**, *94* (9), 441−444.
(31) Cheng, D.; Han, W.; Yang, K.; Song, Y.; Jiang, M.; Song, E. One-step facile synthesis of hyaluronic acid functionalized fluorescent gold nanoprobes sensitive to hyaluronidase in urine specimen from bladder cancer patients. *Talanta* **2014**, *130*, 408−414.
(32) Nossier, A. I.; Eissa, S.; Ismail, M. F.; Hamdy, M. A.; Azzazy, H. M. E.-S. Direct detection of hyaluronidase in urine using cationic gold nanoparticles: A potential diagnostic test for bladder cancer. *Biosens. Bioelectron.* **2014**, *54*, 7−14.
(33) Liu, S.; Zhao, N.; Cheng, Z.; Liu, H. Amino-functionalized green fluorescent carbon dots as surface energy transfer biosensors for hyaluronidase. *Nanoscale* **2015**, *7* (15), 6836−6842.
(34) Wang, Z.; Li, X.; Song, Y.; Li, L.; Shi, W.; Ma, H. An Upconversion Luminescence Nanoprobe for the Ultrasensitive Detection of Hyaluronidase. *Anal. Chem.* **2015**, *87* (11), 5816−5823.
(35) Chib, R.; Mummert, M.; Bora, I.; Laursen, B. W.; Shah, S.; Pendry, R.; Gryczynski, I.; Borejdo, J.; Gryczynski, Z.; Fudala, R. Fluorescent biosensor for the detection of hyaluronidase: intensity-based ratiometric sensing and fluorescence lifetime-based sensing using a long lifetime azadioxatriangulenium (ADOTA) fluorophore. *Anal. Bioanal. Chem.* **2016**, *408* (14), 3811−3821.
(36) Gu, W.; Yan, Y.; Zhang, C.; Ding, C.; Xian, Y. One-Step Synthesis of Water-Soluble MoS2 Quantum Dots via a Hydrothermal Method as a Fluorescent Probe for Hyaluronidase Detection. *ACS Appl. Mater. Interfaces* **2016**, *8* (18), 11272−11279.
(37) Yang, W.; Ni, J.; Luo, F.; Weng, W.; Wei, Q.; Lin, Z.; Chen, G. Cationic Carbon Dots for Modification-Free Detection of Hyaluronidase via an Electrostatic-Controlled Ratiometric Fluorescence Assay. *Anal. Chem.* **2017**, *89* (16), 8384−8390.
(38) Li, X.; Zhou, Z.; Tang, Y.; Zhang, C. C.; Zheng, Y.; Gao, J.; Wang, Q. Modulation of assembly and disassembly of a new tetraphenylethene based nanosensor for highly selective detection of hyaluronidase. *Sens. Actuators, B* **2018**, *276*, 95−100.
(39) Liu, Q.; Yan, X.; Lai, Q.; Su, X. Bimetallic gold/silver nanoclusters-gold nanoparticles based fluorescent sensing platform via the inner filter effect for hyaluronidase activity detection. *Sens. Actuators, B* **2019**, *282*, 45−51.

DOI: 10.1021/acsabm.9b01082
ACS Appl. Bio Mater. 2020, 3, 1158−1164

(40) Kim, J. W.; Kim, J. H.; Chung, S. J.; Chung, B. H. An operationally simple colorimetric assay of hyaluronidase activity using cationic gold nanoparticles. *Analyst* **2009**, *134* (7), 1291−1293.
(41) Shen, M. Y.; Chao, C. F.; Wu, Y. J.; Wu, Y. H.; Huang, C. P.; Li, Y. K. A design for fast and effective screening of hyaluronidase inhibitor using gold nanoparticles. *Sens. Actuators, B* **2013**, *181*, 605−610.
(42) Li, Z.; Tang, C.; Huang, D.; Qin, W.; Luo, F.; Wang, J.; Guo, L.; Qiu, B.; Lin, Z. Sensitive Hyaluronidase Biosensor Based on Target-Responsive Hydrogel Using Electronic Balance as Readout. *Anal. Chem.* **2019**, *91* (18), 11821−11826.
(43) Li, Z.; Chen, H.; Zhuo, Z.; Huang, D.; Luo, F.; Chen, L.; Wang, J.; Gun, L.; Qiu, B.; Lin, Z. Electrochemiluminescence biosensor for hyaluronidase activity detection and inhibitor assay based on the electrostatic interaction between hyaluronic acid and Ru(bpy)(3)(2+). *Sens. Actuators, B* **2018**, *275*, 409−414.
(44) Wang, D.; Li, Y.; Lin, Z.; Qiu, B.; Guo, L. Surface-Enhanced Electrochemiluminescence of Ru@SiO2 for Ultrasensitive Detection of Carcinoembryonic Antigen. *Anal. Chem.* **2015**, *87* (12), 5966−5972.

DOI: 10.1021/acsabm.9b01082
ACS Appl. Bio Mater. 2020, 3, 1158−1164